

A Novel Fast Switching Photonic Phase Shifter for Ka-Band

Praveena P.G¹, Ugra Mohan Roy², Rohini Deshpande³

^{1,2} Faculty of Engineering and Technology, M.S. Ramaiah University of Applied Sciences, Bengaluru

³Reva University, Bengaluru

e-mail: praveenpg030@gmail.com

Abstract

Photonic phase shifters for Ka-band have been used in satellite communication and in many other communication systems. In these applications speed, bandwidth, power consumption and size have become more significant. In communication systems beamforming with fast switching phase shifters has special importance for Ka band. Integrated microwave photonics allow the implementation of phase shifters. We propose a novel architecture for photonic phase shifter with switching time of about 30 to 52 fs .as compared to existing architecture. The phase shifter architecture has been designed with DC tunable ring resonator, S-bend waveguide switch and nanowire DC tunable phase shifter. The designed nanowire waveguide for DC tunable ring resonator, S-bend waveguide switch and DC tunable phase shifter has been simulated using OptiFDTD as well as with MATLAB.

KeyWords: Integrated Microwave Photonics (IMWP), True Time Delays (TTD), Phase Shifter, Radio Frequency (RF), Waveguides

1. INTRODUCTION

Phase shifter design using Integrated Microwave Photonics (IMWP) is one of the exciting areas of current research. IMWP is microwave technology based on photonics. In communication systems large bandwidth is one of major requirement and antenna beamforming has special importance. For antenna beamforming, IMWP signal processing techniques allow the implementation of True Time Delays (TTD) or phase shifters. The phase shift of microwave signals is achieved in the optical domain for optical beamforming [1]. In MWP RF signal is processed in optical domain and then it is reconvertd into RF signal. In this case processing of optical signal is through photonic phase shifter. RF to optical signal conversion is through modulator and laser. Optical to electrical conversion is through photodetector. As per the exixting literature the phase shifter switching time of <1 ns is required for higher bands, but the design and simulation of photonic phase shifter for Ka-band with minimum switching time has not been explored [2,3]. In this paper we have proposed and designed an optical phase shifter for Ka band. The designed phase shifter consists of DC tunable ring resonator, different lengths of S-bend waveguides and DC tunable linear waveguide phase shifter.

1.1 Fast Switching Phase Shifter

In this section the proposed block diagram of the fast switching phase shifter has been discussed. The components of fast switching phase shifter includes Laser source, MZ Modulator, DC tunable Ring Resonator, Linear and S-bend waveguides, and photodetector. The

fast switching time of 52 fs achieved with newly designed S-bend. Phase shifter arms also designed with linear waveguide DC tuning, which gives a wide band phase shift of 0 to 360 degree. Phase shifted optical signal converted into RF signal by coherent photodetection technique. Photodetector output is an electrical signal, which is fed into linear antenna arrays. Fig.1 shows the block diagram of photonic phase shifter for Ka-band. Range of frequencies lying in Ka-band is 26 GHz – 40 GHz. Laser source of carrier 193.55 THz used. Hence carrier for RF signal is optical carrier which is a very high frequency. The conversion from RF signal to terra Hertz signal achieved by Mach-Zehnder modulator. Modulated signal has multiple wavelength along with the carrier containing message signal.

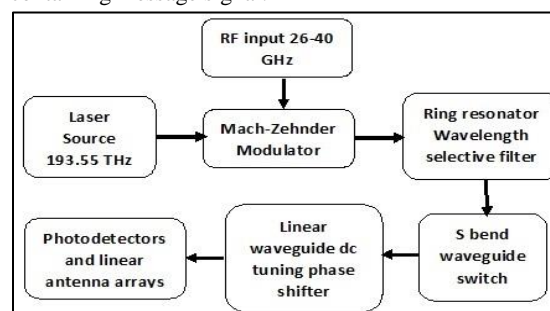


Fig. 1 Block Diagram of Photonic Phase Shifter for Ka-Band

1.2 Design and Simulation of Fast Switching Phase Shifter

The designed phase shifter consists of nanowire DC tunable ring resonator, S-bend waveguide switch and DC tunable phase shifter. The ring resonator used to filter out

the desired wavelength which is achieved by varying coupling coefficient and ring radius [4]. The ring resonator designed with nanowire ring waveguide radius of 2.23175 μm . The short laser pulse yields wider bandwidth for communication systems [5]. Hence the ring resonator designed for 15 fs half width and 100 fs Gaussian Modulated Continuous Wave (GMCW). Use of compact silicon based microring resonator enables high bandwidth tuning [6]. To achieve confinement of light in waveguide, Si core should have minimum 200 nm thickness [7]. The confinement also depends on Si core width, if its width <400 nm evanescent field increases [8]. The ring resonator has Si core width of 415 nm and channel thickness of >200 nm. The phase shifter based on single ring resonator with a tunable Mach-Zehnder interferometer for wide range of band can be used [9]. But the design based on micro heater over waveguide introduces thermal crosstalk and tuning requires distance between successive micro heaters. Instead of this method, When DC voltage is applied across p and n doped nanowire or ring resonator, effective refractive index of Si waveguide changes [10]. The effective refractive index of waveguide placed at coupling region of ring resonator is tunable as shown in Fig.2. Effective index of waveguide could be tunable with DC voltage. The waveguide proposed for two electro-optic materials. First one is p and n doped nanowire waveguide and the second being LiNbO₃ waveguide. Similarly DC tuning is possible on LiNbO₃ waveguide with overlaid electrodes placed at the coupling region. Fig.3 shows optical spectrum of ring resonator drop port output for GMCW signal is at 1.54979 μm . It shows that, at 1.54979 μm wavelength (which corresponds to 26 GHz signal along with optical carrier) optical power is maximum. Hence the required wavelength is filtered out using ring resonator. The corresponding $n_{\text{effcouple}}$ value is tabulated. Similarly design is simulated over Ka-band and corresponding $n_{\text{effcouple}}$ values are tabulated as given in Table 1. The polymer S-bend arc waveguide has low bending loss [11]. The bending loss in dBm calculated as difference between power at starting of bend waveguide and power at end of bend waveguide [12].

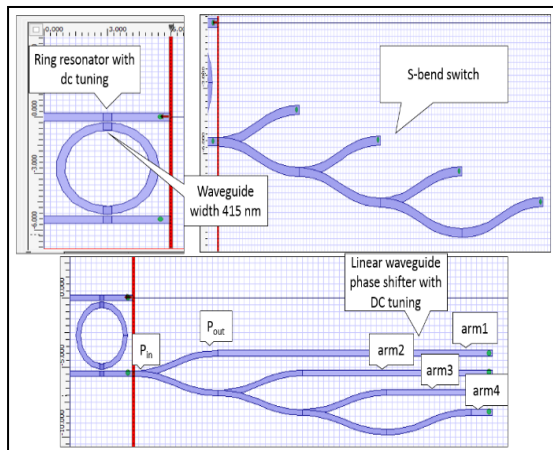


Fig. 2 DC Tunable Ring Resonator, S-Bend Waveguide Switch and Phase Shifter

1.3 S-bend and Linear Waveguides for Fast Switching

For S-bend waveguide with associated radius of 11.3 μm , Si core width of 415 nm, channel thickness is >150 nm, bending loss is found to be -0.56 dBm.

$$t_{\text{arm}} = \frac{d}{c/n_{\text{eff}}} \dots \dots \dots (1)$$

Using Eq. 1 and Fig.2, delays in optical power introduced at the arms of S-bend waveguides depends on length (d) of S-bend waveguides. The difference between delays in successive arms gives switching time for phase shifter, which are extended from s-bend waveguide arms. Light velocity c, effective refractive index n_{eff} chosen such that optical power loss is minimum. The S-bend waveguide has very less bending loss. Hence this time shift is used to switch phase shifting. S-bend waveguide switching time for phase shifter using OptiFDTD found to be 30 fs. The switching time for phase shifter also calculated for Ka-band using MATLAB, which is found to be 52 fs. For Ti: LiNbO₃ waveguide change in effective index value after applying voltage is positive. To get positive change in refractive index from original refractive index of LiNbO₃ 2.14, titanium is diffused to LiNbO₃ waveguide.

$$\delta\phi = \phi_0 \mp \frac{\pi r n_1^3 V L}{2 d} \dots \dots \dots (2)$$

As shown in Eq.2, the tunable phase depends on initial phase ϕ_0 , initial refractive index n_1 , voltage (V), linear waveguide length (L) and electrodes gap (d) from linear waveguide. The end of linear waveguides of each arms are maintained at same point with respect to y-axis. This is to couple arms of phase shifter and photodetector using single mode fiber without disturbing phase excitation values. Effective refractive index of 3 for 4 arms of the phase shifter gives phase shift of 60°. Fig.2 also shows optiFDTD design of DC tunable phase shifter. Linear waveguides of arm1, arm2, arm3 and arm4 designed with initial effective refractive index of 3. Change in phase due to electro-optic effect or Pockels effect, as in [13]. Optical spectrum for DC tunable ring resonator drop port for 26GHz input RF signal is shown in Fig.3.

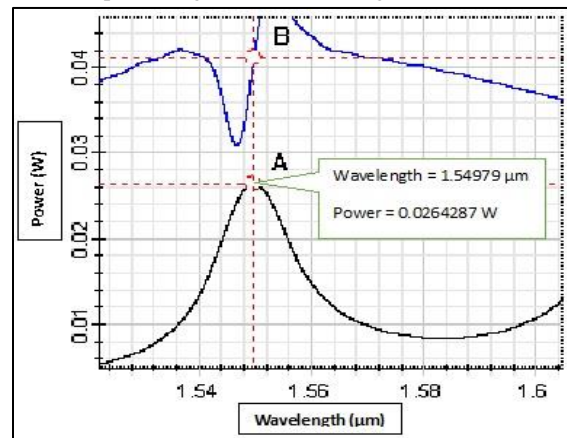


Fig. 3 DC Tunable Ring Resonator Drop Port Optical Spectrum for 26 GHz Input RF Signal

Fig.4 shows delay in arms of phase shifter for Ka-band simulated using MATLAB, by analytical approach. Fig.5

shows the optical power at 1.54979 μm is 0.0356448 W. The power at arm1 and input power is observed to be same. On the other arms the tapped optical power lies between 0.02 W to 0.01 W, which are detectable optical power for photodetector.

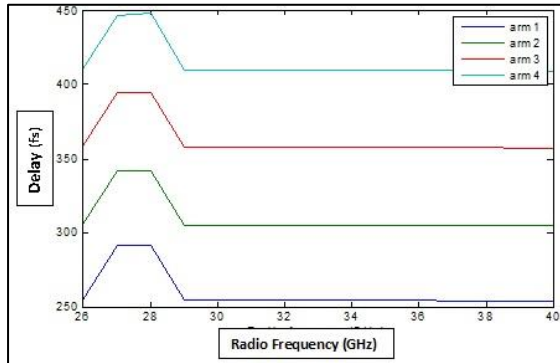


Fig. 4 Delay in arms of phase shifter for Ka-band

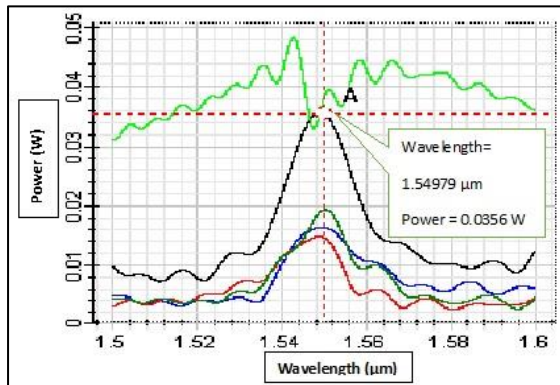


Fig. 5 Optical spectrum of 4 arms of the phase shifter at 26 GHz RF signal input

Fig.6 shows phase excitations at 4 arms of the phase shifter. From the phase excitation values phase shift between successive arms have been calculated. The phase shift of 60° have been obtained for Ka-band. OptiFDTD optical spectrum of phase shifter for Ka-band RF signal have been verified.

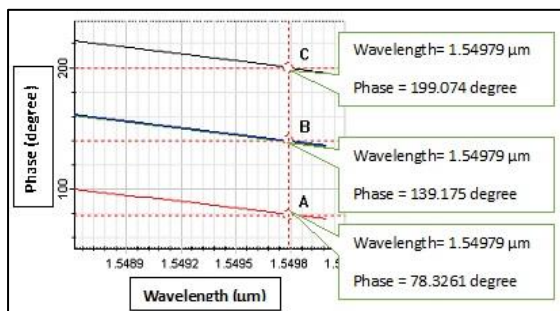


Fig. 6 Phase excitations at arms of phase shifter for modulated center wavelength 1.54979 μm

2. RESULTS AND DISCUSSIONS

Table 1. shows DC tunable phase shifter results. For Ka-band range of radio frequencies center wavelength of modulated signal is calculated. Ring resonator initially designed with nanowire waveguide of Si core width of 415 nm, channel thickness >150 nm. Then instead of

changing ring radius to filter out center wavelength for different frequencies, a p-i-n typed nanowire waveguide or LiNbO_3 waveguide with width of 415 nm is placed at coupling region of linear waveguide and ring waveguide.

Table 1. DC tunable ring resonator

RF Ka-band (GHz)	Wave-Length (μm)	Nanowire Effective refractive index n_{eff}	Effective index coupling region $n_{\text{effcouple}}$	Voltage required (V) for Phase shifter
26	1.5497918	2.29859	2.0105	68.28
27	1.5497838	2.298603	2.0085	69.34
28	1.5497758	2.29860	2.0085	69.34
29	1.5497678	2.29862	2.0077	69.75
30	1.5497598	2.29863	2.0068	70.23
31	1.5497518	2.29864	2.0063	70.49
32	1.5497438	2.29866	2.0059	70.71
33	1.5497358	2.29866	2.0056	70.86
34	1.5497278	2.29867	2.0055	70.91
35	1.5497198	2.29868	2.0054	70.97
36	1.5497118	2.29870	2.0052	71.08
37	1.5497038	2.29871	2.0045	71.44
38	1.5496957	2.29871	2.0040	71.71
39	1.5496877	2.29872	2.0035	71.97
40	1.5496797	2.29874	2.0030	72.24

Effective refractive index of this nanowire waveguide at coupling region changed to filter out center wavelength. Effective refractive index of coupling region $n_{\text{effcouple}}$ for which center wavelength is tuned is obtained from OptiFDTD, results are tabulated in table1. If LiNbO_3 waveguide material placed in coupling region, then voltage required to get $n_{\text{effcouple}}$ is calculated using MATLAB considering ‘‘Pockels effect ‘‘.

Table 2. OptiFDTD result of phase shifter for Ka-band

RF Ka-band (GHz)	Phase at arm1 ϕ_1°	Phase at arm2 ϕ_2°	Phase at arm3 ϕ_3°	Phase at arm4 ϕ_4°
26	199.074	139.175	78.6603	139.175
27	199.216	139.957	77.8315	139.957
28	200.197	139.336	79.4107	139.336
29	201.538	139.169	78.5559	139.169
30	200.925	139.637	79.056	138.637
31	199.942	138.329	79.85	138.329
32	198.608	139.421	78.4926	139.421
33	199.835	140.697	78.1312	140.697
34	199.831	140.208	79.6531	140.208
35	200.341	139.227	79.6025	139.227
36	200.949	140.855	79.902	140.855
37	200.617	140.793	79.2097	140.793
38	199.763	140.964	79.1751	140.964
39	200.352	140.229	78.1967	140.229

40	200.642	140.537	79.395	140.537
----	---------	---------	--------	---------

Table 2. shows OptiFDTD results of phase shifter for Ka-band. For Ka-band radio frequencies phase excitation values for corresponding center wavelength at 4 arms of the phase shifter are tabulated. From the phase excitation values phase shift between successive arms has been computed. Hence ka band phase shifter is designed to provide 60° phase shift. To obtain other phase shifts the required effective refractive index of 4 arms has to be obtained from OptiFDTD simulations.

Table 3. MATLAB results of S-bend waveguide switch for Ka-band

RF Ka-band (GHz)	Delay at arm1 (fs)	Delay at arm2 (fs)	Delay at arm3 (fs)	Delay at arm4 (fs)
26	254.78	305.88	358.24	410.59
27	291.13	342.18	394.48	446.78
28	291.13	342.18	394.48	447.78
29	254.43	305.46	357.74	410.02
30	254.31	305.32	357.58	409.84
31	254.25	305.24	357.49	409.74
32	254.20	305.18	357.42	409.66
33	254.16	305.14	357.37	409.59
34	254.15	305.12	357.35	409.57
35	254.14	305.11	357.33	409.55
36	254.11	304.08	357.29	409.51
37	254.02	304.97	357.17	409.37
38	253.96	304.89	357.08	409.27
39	253.90	304.82	356.99	409.17
40	253.83	304.74	356.90	409.06

Table 3. shows MATLAB results of S-bend waveguide switch for Ka-band. For Ka-band frequencies the delay values calculated for different arms of S-bend waveguides using mathematical equation for laser, RF signal, MZM, ring resonator and S-bend waveguide. The difference between delay values of successive arms of S-bend waveguide gives switching time for phase shifter. Table 4 shows the comparison of the designed phase shifter with existing architecture.

Table 4. Comparison Table

Parameters	Value, Reference	Proposed architecture
Switch time (s)	1ns [3]	30 fs and 52 fs
Frequency Band (Hz)	10 to 13 GHz [2]	26 to 40 GHz
Phase shifting technique	MRR with micro heater over waveguide [9]	MRR with DC tunable linear waveguide

3. CONCLUSIONS

A photonic phase shifters for ka band has been designed using nanowire DC tunable ring resonator, S-bend and linear waveguides switch with the switching time of about 30 to 52 fs. Phase shift of 60° has been achieved between successive arms of designed ka band optical phase shifter. The phase shifter can be further tuned for wide range of angles.

REFERENCES

- [1] Iezekiel, S., Burla, M., Klamkin, J., Marpaung, D. and Capmany, J., 2015. RF engineering meets optoelectronics: Progress in integrated microwave photonics. *IEEE Microwave Magazine*, 16(8), pp.28-45.
- [2] Burla, M., 2013. Advanced integrated optical beam forming networks for broadband phased array antenna systems.
- [3] Vidal, B., Mengual, T. and Martí, J., 2012. Fast optical beamforming architectures for satellite-based applications. *Advances in Optical Technologies*, 2012.
- [4] Bogaerts, W., De Heyn, P., Van Vaerenbergh, T., De Vos, K., Kumar Selvaraja, S., Claes, T., Dumon, P., Bienstman, P., Van Thourhout, D. and Baets, R., 2012. Silicon microring resonators. *Laser & Photonics Reviews*, 6(1), pp.47-73.
- [5] Lemus, D., 2011. Laser source for UWB pulse generation.
- [6] Cardenas, J., Foster, M.A., Sherwood-Droz, N., Poitras, C.B., Lira, H.L., Zhang, B., Gaeta, A.L., Khurgin, J.B., Morton, P. and Lipson, M., 2010. Wide-bandwidth continuously tunable optical delay line using silicon microring resonators. *Optics express*, 18(25), pp.26525-26534.
- [7] Selvaraja, S.K., 2011. *Wafer-scale fabrication technology for silicon photonic integrated circuits* (Doctoral dissertation, PhD thesis, Ghent University).
- [8] Shi, Y., Ma, K. and Dai, D., 2016. Sensitivity enhancement in Si nanophotonic waveguides used for refractive index sensing. *Sensors*, 16(3), p.324.
- [9] Chew, S.X., Huang, D., Li, L., Song, S., Tran, M.A., Yi, X. and Bowers, J.E., 2019. Integrated microwave photonic phase shifter with full tunable phase shifting range (> 360°) and RF power equalization. *Optics express*, 27(10), pp.14798-14808.
- [10] Watts, M.R., Trotter, D.C., Young, R.W. and Nielson, G.N., National Technology and Engineering Solutions of Sandia LLC, 2009. *Wavelength-tunable optical ring resonators*. U.S. Patent 7,616,850.
- [11] Kruse, K.L. and Middlebrook, C.T., 2015. Fan-out routing and optical splitting techniques for compact optical interconnects using single-mode polymer waveguides. *Journal of Modern Optics*, 62(sup2), pp.S1-S10.
- [12] Musa, S.M. ed., 2013. Computational nanophotonics: modeling and applications. *CRC Press*.